



Application of new waveform analysis methods reflecting F-wave diversity -classification of F-wave diversity according to differences in the derived muscles

Marina Todo^{a,b,*}, Toshiaki Suzuki^{a,b}, Masaaki Hanaoka^c, Hitoshi Asai^d

^a Department of Physical Therapy, Faculty of Health Sciences, Kansai University of Health Sciences, 2-11-1, Wakaba, Sennangun, Kumatori, Osaka, Japan

^b Graduate School of Health Sciences, Graduate School of Kansai University of Health Sciences, 2-11-1, Wakaba, Sennangun, Kumatori, Osaka, Japan

^c Department of e-Health Science, Graduate School of Medicine, Shinshu University, 3-1-1, Asahi, Matsumoto City, Nagano, Japan

^d Department of Physical Therapy, Graduate Course of Rehabilitation Science, School of Health Sciences, College of Medical, Pharmaceutical, and Health Sciences, Kanazawa University, 5-11-80, Kotatsuno, Kanazawa City, Ishikawa, Japan

ARTICLE INFO

Keywords:

F-wave diversity
Histogram
Waveform analysis
Tibial nerve
F-wave parameter

ABSTRACT

Background: The F wave waveforms show diversity according to the number and size of re-firing cells, but there is still no analytical method that reflects this feature. We previously reported that five classifications of F waves are obtained from the ulnar nerve. However, the diversity of F waves derived from the lower extremities may not be similar. We therefore compared the diversity of F waves in the upper and lower extremities in healthy subjects.

New method: F waves were measured during tibial nerve stimulation in 26 healthy subjects. The amount of amplitude decrease was calculated from the amplitude value after the additive averaging process and based on the average amplitude value of each stimulus, and the relationship between the peak latency and density was examined.

Results: The amount of amplitude decrease due to the additive averaging process was negatively correlated with the density of negative peaks. The diversity of F waves could be categorized into four class based on the histograms.

Comparison with existing method: The new method uses a novel additive average method that reflects the diversity of F waves. Furthermore, it uses a histogram to visualize the cancellation between waveforms.

Conclusion: We developed an analysis method that reflects the diversity of F waves in a novel manner, which visualizes cancellation between waveforms using a histogram.

1. Introduction

The F wave is a small waveform emitted by the dominant muscle caused by the spinal cord anterior horn cells re-firing when the

* Corresponding author. Department of Physical Therapy, Faculty of Health Sciences, Kansai University of Health Sciences, 2-11-1, Wakaba, Sennangun, Kumatori, Osaka, Japan.

E-mail addresses: todo@kansai.ac.jp (M. Todo), suzuki@kansai.ac.jp (T. Suzuki), mhanaoka@shinshu-u.ac.jp (M. Hanaoka), asai@mhs.mp.kanazawa-u.ac.jp (H. Asai).

<https://doi.org/10.1016/j.heliyon.2023.e20551>

Received 27 June 2022; Received in revised form 22 September 2023; Accepted 28 September 2023

Available online 29 September 2023

2405-8440/© 2023 Published by Elsevier Ltd.

This is an open access article under the CC BY-NC-ND license

(<http://creativecommons.org/licenses/by-nc-nd/4.0/>).

alpha motor neuron is electrically stimulated. F waves are characterized by the fact that they are synthesized and have diverse shapes, depending on the size and timing of the anterior horn cells of the spinal cord, which re-fire [1].

In healthy individuals, it is normal for various motor units to be able to fire, and various waveforms can be recorded in the F wave. However, in patients with amyotrophic lateral sclerosis, wherein the numbers of cells in the anterior horn of the spinal cord are decreased, and in cases of stroke with spasticity due to the loss of function of the upper motor neurons, it has been reported that a waveform called Repeater F—which is identical in amplitude, waveform shape, and latency—appears [2–4]. Repeater F has been shown to increase in frequency as the degree of spasticity becomes more severe. However, the number of waveform classifications increases with improvement in voluntary control [5,6] (Fig. 1). Furthermore, in their discussion of this previous study, Suzuki et al. stated that the appearance of Repeater F in individuals with spasticity is due to the firing of only some of the anterior horn cells of the spinal cord. The improvement in voluntariness and muscle tone indicates that the various anterior horn cells of the spinal cord are now ready to fire, which may serve as a future neurophysiological measure of hand dexterity. Besides, the F wave reflects the motor unit, and even when muscle weakness occurs due to a decrease in motor units caused by aging, the evaluation of this F wave waveform is expected to be useful in approaches that lead to the prevention of decline in physical function. Thus, many researchers have stated the importance of analyzing F wave waveforms, as they can be used to evaluate spasticity and voluntariness, in addition to providing clues regarding the state of the anterior horn cells of the spinal cord that make up the F wave [6–8]. However, analyzing F wave waveforms has been difficult due to the complexity of the waveform amplitude values, latency, and shape changes (henceforth referred to as their “diversity”).

We focused on the additive averaging method [9–12], which has been used in the past to simplify analyses, in order to quantify the diversity of F wave waveforms. If the waveforms show diversity, they will cancel each other out, and the amplitude will decrease when the additive averaging process is applied. We hypothesized that the amount of decrease in this amplitude would reflect the diversity of the waveform. Therefore, we first calculated the amount of the amplitude decrease via additive averaging of the F wave derived from the abductor pollicis brevis by median nerve stimulation. Two factors were expected to be responsible for the decrease in amplitude: the persistence of the F wave and the variation in peak latency [13]. To quantify the diversity of F wave waveforms based on these two factors, it is necessary to clarify the relationship between the variation in peak latency and the amount of the amplitude decrease by the additive averaging process.

In a subsequent study, we examined the ulnar nerve, where the persistence of F waves was 80–100%, excluding the factor of reduction due to persistence, but no relationship was found between the variation in peak latency and the amount of reduction in amplitudes by additive averaging. However, on observing the characteristics of individual waveforms, it became clear that there were five main classes, even among the waveforms that showed diversity [14]. Considering the mechanism underlying F wave generation, the characteristics of the waveform are expected to vary depending on the characteristics of the muscle from which it is derived and the percentage of motor units of the innervating nerve. Therefore, it is unlikely that the five classes identified from the ulnar nerve would be applicable to all covered nerves. In addition, it is possible that there is diversity unique to each subject nerve, making it important to understand the characteristics of each subject nerve when analyzing F wave waveforms.

In the present study, the tibial nerve, which can be derived from the lower extremity, is used to derive the F wave from the abductor

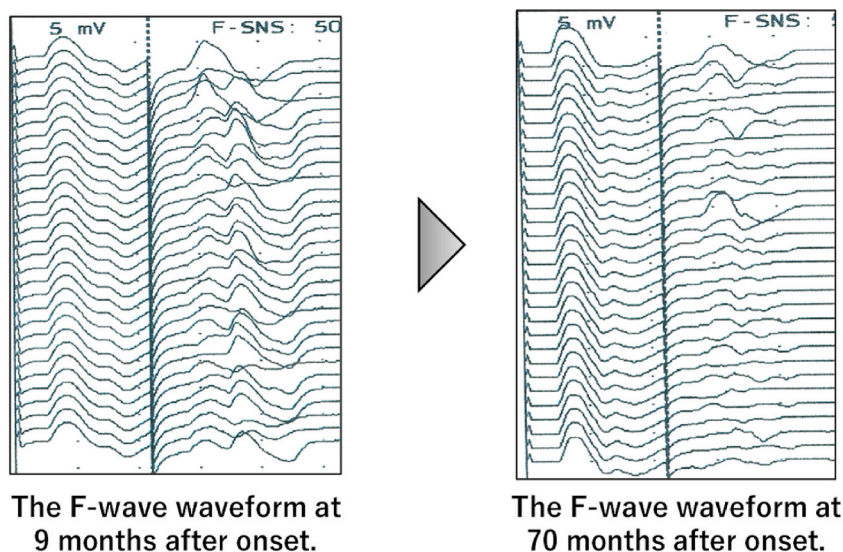


Fig. 1. F-wave changes with improvement in voluntariness.

F-wave measurements of cerebrovascular patients at 9 and 70 months showed 6 to 16 classes of F-wave waveforms, along with improvement in voluntariness and muscle tone. (This figure was published in *Int J Neurorehabilitation*, Eng 3:2, Suzuki T, Bunno Y et al., F-Wave Waveform Values Based On the Correlation Coefficient of Each Waveform Increased Following Improved Voluntary Movements in a Patient with Cerebrovascular Disease: A Case Study with Long-Term Follow-Up, 1000206, 2016).

pollicis brevis. The purpose of this study was to categorize the various types of classification based on the amount of the amplitude decreases when additive averaging was applied, as in the case of the ulnar nerve, along with the characteristics of the peak latency. It also clarified the unique diversity of the tibial nerve. In our experience, F waves obtained by tibial nerve stimulation tend to be larger in amplitude and more complicated than those of the upper limb. In many cases, relatively sharp negative waves appear at a certain latency. Therefore, we hypothesized that the F waves obtained via tibial nerve stimulation would have a higher density of peak latency and a smaller reduction in amplitude due to the additive averaging process in comparison to F waves obtained via upper extremity nerve stimulation.

2. Materials and methods

2.1. The a priori power analysis

Power analysis was conducted using G*power software program (version 3.1.9.4) with the following parameters: Correlation Point biserial model, effect size = 0.5, α error = 0.05, Power (1- β) = 0.8. As a result, the calculated required sample size of this study was 26.

2.2. Participants

Twenty-six healthy subjects (male, n = 13; female, n = 13), mean age 23.0 ± 2.7 years, gave their consent to participate in this study. The left lower limb was measured, and F waves were derived from the 26 unified limbs.

According to the Declaration of Helsinki, we carefully explained the significance and purpose of this study to all of the subjects, and clearly obtained their written consent. This study was approved by the Kanazawa University Medical Ethics Review Committee (approval number: 956-1) and the Kansai University of Health Science Research Ethics Review Committee (approval number: 19-54).

2.3. The F wave test

Regarding the F wave measurement method, after the subject rested in the supine position, the tibial nerve on the non-dominant hand side was electrically stimulated in the basic anatomical limb position, and F waves were measured from the dominant muscle, the abductor hallucis muscle. At this time, the muscles to be measured were palpated to check for the presence of abnormal muscle activity. The participants were asked to experience the intensity of the electrical stimulation and to confirm that it would not cause pain before measurement. The room temperature was set at 25 °C. The F waves were carefully measured using the electromyograph Viking Quest Ver. 9.0. For this study, the frequency range was 20 Hz to 3 kHz, and the sampling frequency was 10 kHz. Regarding the stimulation conditions, a frequency of 1 Hz, a stimulation time of 0.2 msec, an intensity of supramaximal stimulation (1.2 times the intensity at which the maximum amplitude of the M wave was obtained), and 30 stimulations were thus obtained. The stimulating electrode was a bipolar electrode for the recording conditions. An Ag/AgCl electrode with a diameter measuring 1 cm was used as the recording electrode. The recording electrode was placed on the abductor hallucis muscle, the reference electrode was placed on the proximal phalanx of the great toe, the stimulating electrode was placed to stimulate the tibial nerve from the medial malleolus, and the ground electrode was placed between the recording and stimulating electrodes (Fig. 2). The obtained F waves were compared with the persistent F wave appearance, which indicates the ratio of F waves that appeared to the number of stimuli, and the amplitude was calculated via two methods (the additive average method and the average value calculation method). After calculating the changes in amplitude obtained from the two amplitude calculation methods and the density of peaks used in previous studies^{13,14}, the correlation coefficient between the change in amplitude and the peak density was calculated.

The F waves measured from the subjects were visually confirmed on the monitor of a VikingQuest system at 500 μ V/division. The amplitude of F waves that could be visually confirmed was calculated peak-to-peak. The F/M amplitude ratio in this study was then calculated for each individual waveform by dividing by the M wave which was obtained at the supramaximal stimulus ("maximum M wave"). The minimum amplitude was set at 30 μ V based on previous studies^{6,8}. Waveforms that did not meet this criterion were not F

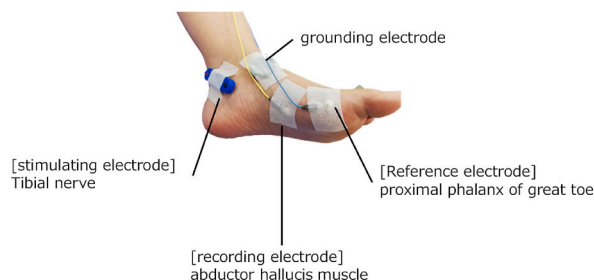


Fig. 2. Electrode attachment position.

The recording electrode was placed on the abductor hallucis muscle, the reference electrode was placed on the proximal phalanx of the great toe, the stimulating electrode was placed to stimulate the tibial nerve from the medial malleolus, and the ground electrode was placed between the recording and stimulating electrodes.

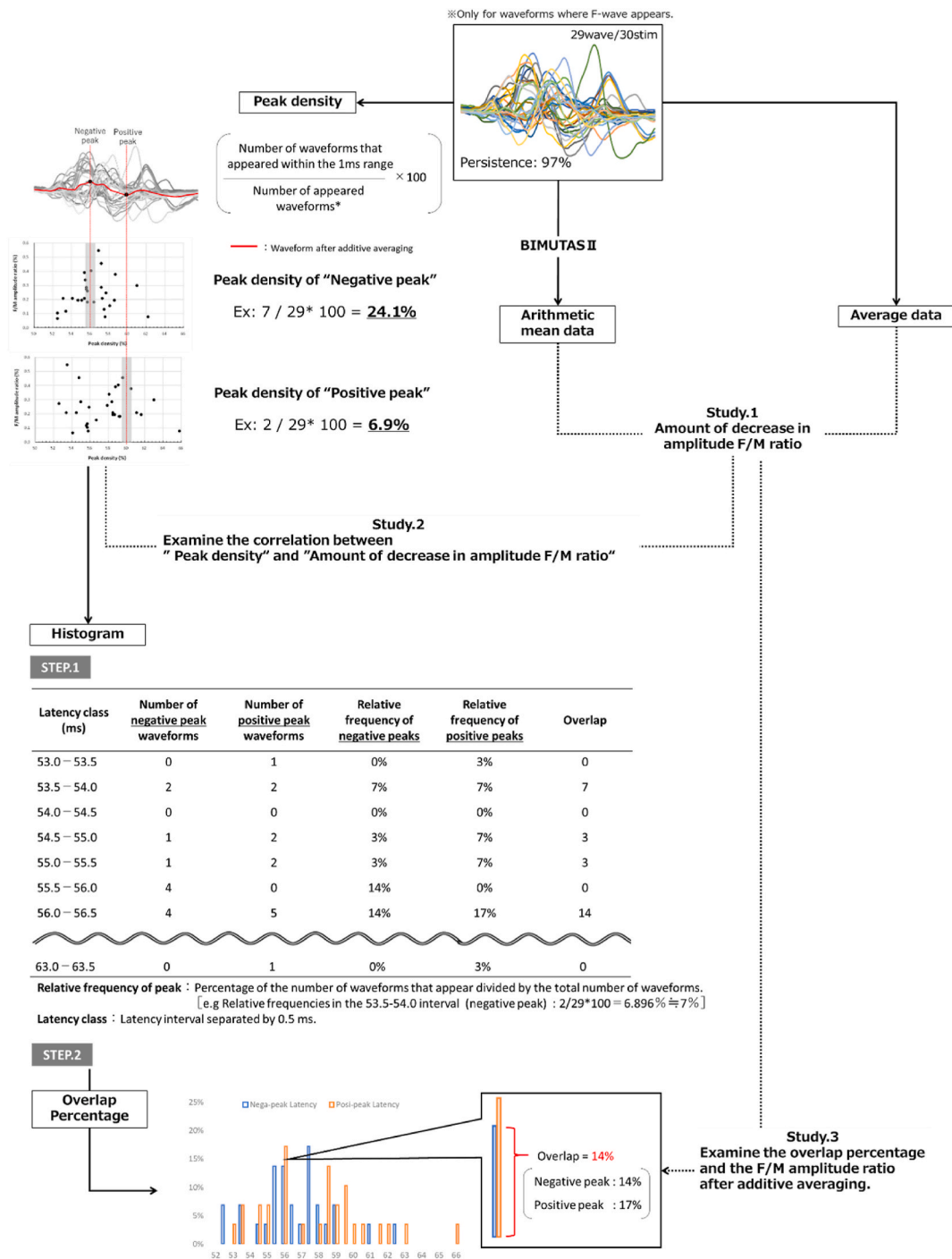


Fig. 3. Flow of the analysis and research.

The amount of amplitude decrease was calculated from the amplitude after the additive averaging process (arithmetic mean data) and the average amplitude (average data) of each stimulus. From these two values, we determined the amount of decrease in the amplitude due to the additive averaging process (Study 1). The number of waveforms that appeared 0.5 msec before and after the peak latency of the waveform after the additive averaging process was calculated as a percentage. The correlation coefficient was then used to examine the relationship between the amplitude and the amount of the amplitude decrease obtained in Study 1 (Study 2). Peak density was visualized in a histogram. To quantify the effect of waveform cancellation, overlap percentages were calculated and compared to the F/M amplitude ratio after additive averaging (Study 3).

waves. Two steps were performed to calculate the amplitude and the amount of change in amplitude due to the additive averaging process. In the first step, the average value of the F/M amplitude ratio (“average data”) of the waveform in which the F wave appeared was calculated. In the second step, additive averaging of waveforms in which F waves appeared was first performed using the BIMUTAS II software program (KISSEICOMTEC, Inc., Nagano, Japan) in order to calculate the average waveform (“arithmetic mean data”). Next, the amplitude obtained from the negative and positive peaks of the arithmetic mean data was used as the amplitude of the F wave, and the F/M amplitude ratio was calculated.

2.4. Data analyses

The flow of the analysis is described below. First, we determined the decrease in the amplitude due to the additive averaging process. We compared the arithmetic mean data with the average data and calculated the decrease in the F/M amplitude ratio by the additive average process. Second, we calculated the latency of the negative and positive peaks from a single waveform obtained by the additive averaging process. To calculate the density of the peak latency, we set an interval of ±0.5 msec of peak latency calculated from the waveform after additive averaging and calculated the number of peaks appearing in the interval as a percentage. This approach calculated how many waveform peaks were densely packed within 0.5 msec before and after the latency of the peaks obtained from the additive averaging process as a percentage for each negative and positive peak (“peak density”) (Fig. 3). We hypothesize that if the peaks appeared within a certain latency, the additive averaging process would have less of a canceling effect, and as a result, the amount of decrease in the F/M amplitude ratio obtained in the first step would be smaller.

In this study, we examined the effect of the additive averaging process on the amplitudes by comparison with the average data (Study 1). Next, to study the canceling effect caused by the diversity of peak latency during the additive averaging process, we compared the amount of decrease in the F/M amplitude ratio by the additive averaging process with the peak density (Study 2). In addition, to visualize the density of the peak latency and clarify the characteristics of individual waveforms, a bar graph of the frequency distribution of the latency of negative and positive peaks was created using a histogram (STEP 1). The data interval of the histogram was set to 0.5-msec increments, and the frequency was the relative frequency obtained by dividing the number of waveforms that appeared in each interval by the total number of waveforms that appeared. In addition, we calculated the value of the overlap between negative and positive peaks (“overlap percentage”) from the histogram to quantify the effect of waveform cancellation (STEP 2). The relationship between the overlap percentage and the F/M amplitude ratio after additive averaging was compared using the correlation coefficient (Study 3). We hypothesize that as the overlap between negative and positive peaks increases, the amount of decrease in the amplitude due to the additive averaging process calculated by Study 1 increases. These studies are expected to prove that two factors, the density of peaks and the overlap of negative and positive peaks, influence the amount of decrease in amplitude value due to additive averaging, and provide basic data for F-waves obtained from the tibial nerve of healthy subjects.

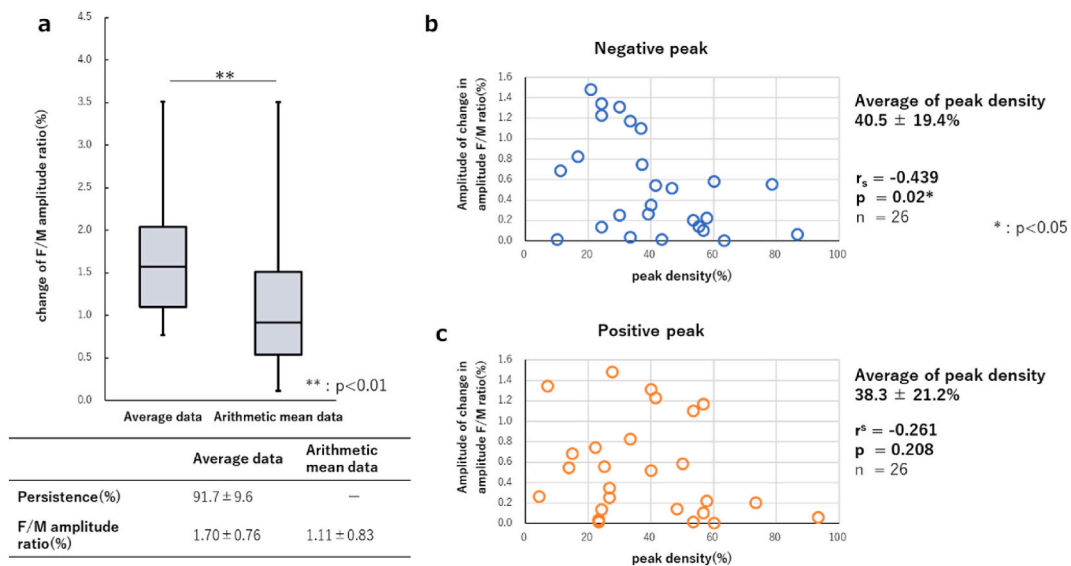


Fig. 4. Relationship between the amount of amplitude decrease by the additive averaging process and the peak density. (a) The upper panel shows box-and-whisker graphs for arithmetic mean data and average data, and the lower panel shows the average Persistence and F/M amplitude ratio for each trial. Regarding the amplitude F/M ratios with the arithmetic mean data and average data, the value with the arithmetic mean data was significantly lower than that with the average data ($p < 0.01$, $r = 0.9$). (b) The mean peak density values were $40.5\% \pm 19.4\%$ for negative peaks. The comparison of the amount of change in the F/M amplitude ratio and the peak density was $r_s = -0.439$ ($p = 0.02$) for negative peaks. (c) The mean peak density values were $38.3\% \pm 21.2\%$ for positive peaks. The comparison of the amount of change in the F/M amplitude ratio and the peak density was $r_s = -0.261$ ($p = 0.208$) for positive peaks.

2.5. Statistical analyses

- Study 1: Comparison of the arithmetic mean data with average data

The Shapiro-Wilk test was used to examine the normality of the amplitude F/M ratio between the arithmetic data and the average data. Since normality was rejected, a nonparametric Wilcoxon's signed rank test was used instead.

- Study 2: Comparison of the amount of change in the F/M amplitude ratio due to peak density and additive averaging

The relationship between the amount of decrease in the F/M amplitude ratio and the peak densities of the negative and positive peaks was compared using Spearman's rank correlation coefficient, and the test of no correlation was performed for the coefficient.

- Study 3: Comparison of the overlap percentage and the F/M amplitude ratio after additive averaging

The relationship between the overlap percentage of negative and positive peaks and the F/M amplitude ratio calculated from the waveform after additive averaging was compared using Spearman's rank correlation coefficient, and a test of no correlation was performed for the coefficient.

The significance level was set at <5% in all cases, and all statistical analyses were performed using SPSS (SPSS, Inc., Chicago, IL, USA) version 19.0.

3. Results

3.1. Study 1: comparison of arithmetic mean data with average data

The persistence of F waves in the 26 subjects was $91.7\% \pm 9.6\%$, and the F/M amplitude ratio was $1.70\% \pm 0.76\%$ in the average data and $1.11\% \pm 0.83\%$ in the arithmetic mean data. Regarding the F/M amplitude ratios in the arithmetic mean data and the average data, the value obtained with the arithmetic mean data was significantly lower than that obtained with the average data ($p < 0.01$, $r = 0.9$) (Fig. 4-a).

3.2. Study 2: comparison of the amount of change in the F/M amplitude ratio due to peak density and additive averaging

The mean peak density values were $40.5\% \pm 19.4\%$ for negative peaks and $38.3\% \pm 21.2\%$ for positive peaks, which were slightly higher in comparison to those obtained with the ulnar nerve. The correlation between the amount of decrease in the F/M amplitude ratio and the peak density was $r_s = -0.439$ ($p = 0.02$) for negative peaks and $r_s = -0.261$ ($p = 0.208$) for positive peaks, with a significant negative correlation only for negative peaks (Fig. 4-b).

The mean peak density values were $40.5\% \pm 19.4\%$ for negative peaks and $38.3\% \pm 21.2\%$ for positive peaks. The comparison of the amount of change in the F/M amplitude ratio and the peak density was $r_s = -0.439$ ($p = 0.02$) for negative peaks and $r_s = -0.261$ ($p = 0.208$) for positive peaks, with a significant negative correlation only for negative peaks.

3.3. Study 3: comparison of the overlap percentage with the F/M amplitude ratio after the additive averaging process

The mean value of the overlap percentage was $25.4\% \pm 14.2\%$. The correlation coefficient between the overlap percentage and the F/M amplitude ratio after additive averaging was $r_s = -0.648$ ($p < 0.001$), indicating a significant negative correlation. In other words,

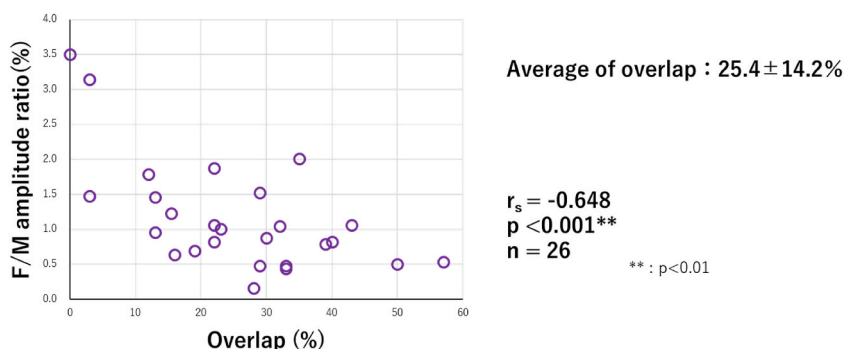


Fig. 5. Relationship between the overlap percentage of negative and positive peaks and the amplitude after the additive averaging process. The mean value of the overlap percentage for each peak was $25.4\% \pm 14.2\%$. The correlation coefficient between the overlap percentage and the amplitude F/M ratio after the additive averaging process was $r_s = -0.648$ ($p < 0.001$), indicating a significant negative correlation.

it was confirmed that the larger the ratio of latency overlap between negative and positive peaks became, the smaller the F/M amplitude ratio became after additive averaging (Fig. 5). As a result of visualizing the density of the peak latency and performing a classification analysis based on the characteristics of the individual waveforms, we were able to categorize the waveforms into three classes, similarly to a previous study related to the ulnar nerve¹⁴⁾ (Fig. 6).

In class 1, the overlap percentage was more than 30%, and the influence of cancellation between waveforms was large, with the

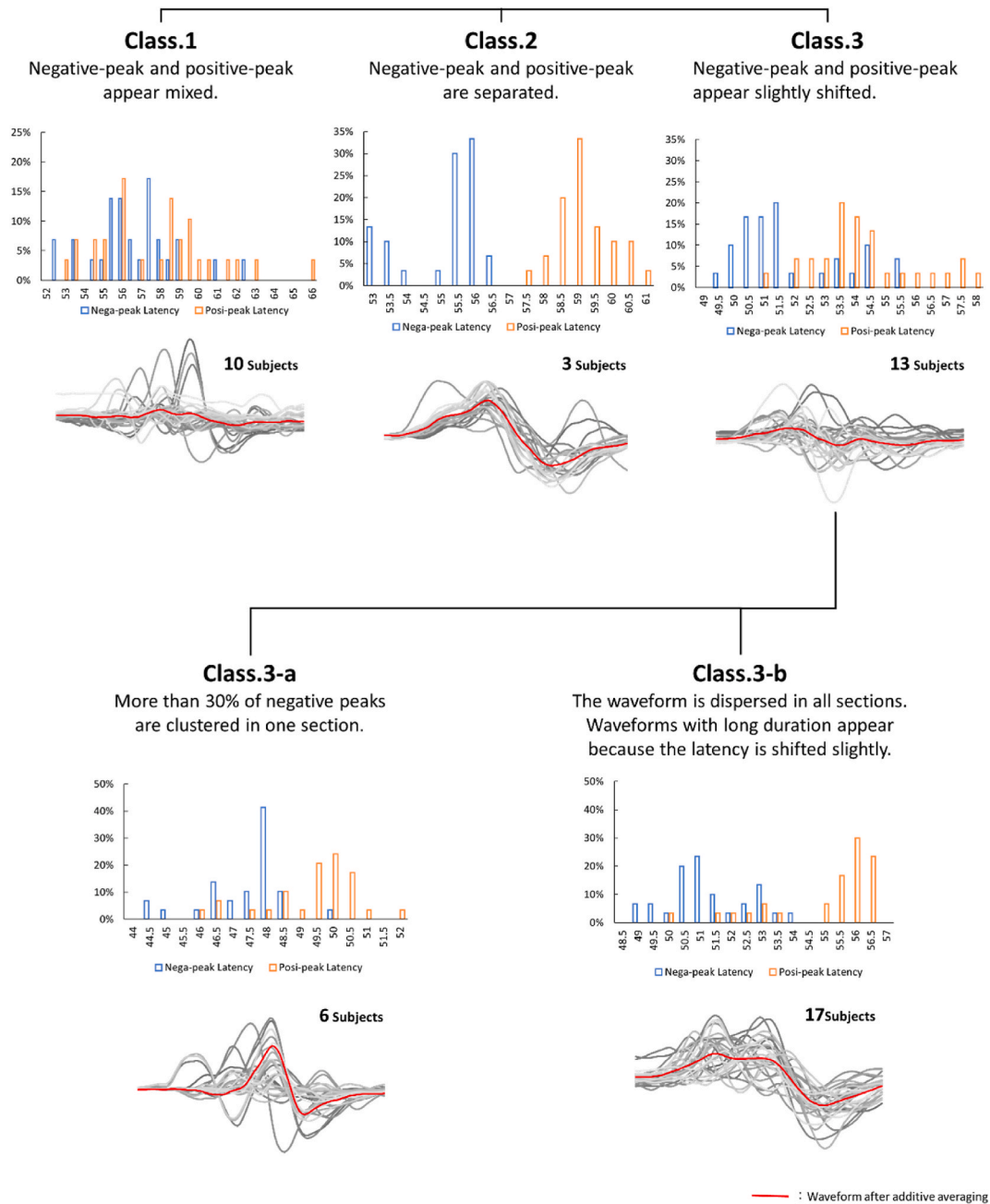


Fig. 6. Class categories of F waves obtained via tibial nerve stimulation using histogram.

Class 1: The overlap percentage is $>30\%$, and the influence of cancellation between waveforms is large, with the waveform close to the baseline after the additive averaging process. Class 2: The overlap percentage is $0\text{--}3\%$, the influence of cancellation between waveforms is small, and many similar waveforms appear, with the amplitude F/M ratio of the waveforms after additive averaging process also being large. Class 3: The overlap percentage ranges from 12% to 29% , with a slight overlap between negative and positive peaks. Class 3a: $\geq 30\%$ of the total negative peaks of the emerged F wave are clustered in one section. Class 3b: The percentage of F waves that are densely packed in one section of the histogram is $<30\%$, and the latency of each peak is dispersed in a wide range.

waveform close to the baseline after additive averaging. Ten patients were classified into this category. In class 2, the overlap percentage was 0–3%, and the influence of cancellation between waveforms was small, with relatively similar waveforms appearing in many cases. As a result, the waveform after additive averaging also had a large F/M amplitude ratio. Three patients were classified into this category. In class 3, the overlap percentage was 12–29%, with a slight overlap between negative and positive peaks, and 13 patients were classified into this category. Among the 13 subjects who were classified into class 3, when we focused on the peak density of negative peaks that affected the amplitudes after the additive averaging process suggested in Study 2, we were able to classify these patients into two categories based on the histogram and waveform characteristics. Six patients were classified into class 3a, in which the negative peaks accounting for more than 30% of the total F waves that appeared were clustered into a single section (highest density in a section was 64%), while 7 patients were classified into class 3b, in which the percentage of density in a single section of the histogram was <27%, and the overall latency of each peak was dispersed. When we checked the raw waveforms, we found that waveforms with similar amplitudes appeared with slightly different latencies, and the waveforms obtained by the additive averaging process were not high in amplitude but had a smooth waveform with a long duration. Class 3b corresponded to class 3-3 of the ulnar nerve¹⁴.

4. Discussion

In the present study, we examined the relationship between the amount of amplitude decrease and peak density when additive averaging was applied to the tibial nerve. In addition, we analyzed the waveform classification based on the overlap percentage of negative and positive peaks from the histogram that visualized the density of peak latency. The results suggest that the additive averaging process significantly reduces the amplitudes of the average data and that this factor is related to the peak density of the negative peaks.

In the histogram used to visualize the density of negative peaks, a correlation was observed between the overlap percentage of negative and positive peaks and the amount of amplitude decrease, suggesting that the effect of waveform cancellation, which has been described at the level of discussion, can be objectively quantified. Furthermore, based on the overlap percentage, the tibial nerve could be divided into three classes, similar to the ulnar nerve, and class 3 could be further divided into two subclasses based on the characteristics at the negative peak.

In the present study, we hypothesized that the F waves obtained with tibial nerve stimulation would have a higher density of peak latency and a smaller reduction in amplitude due to the additive averaging process in comparison to those obtained with upper extremity nerve stimulation. This study showed that the peak density in the tibial nerve at both peaks was 7–8% higher than that in the ulnar nerve, and the amount of amplitude decrease of the F/M ratio by the additive averaging process was 0.13% lower than that in the ulnar nerve, which is consistent with our hypothesis. Below, we discuss the following two factors from a neurophysiological point of view [1]: the correlation between peak density and negative peak, and [2] the comparison of waveform classes between the tibial and ulnar nerves.

4.1. Correlation between peak density and negative peak

When examining the correlation between peak density and the amount of amplitude decrease, the negative correlation found here suggests that the amount of amplitude decrease due to the additive averaging process is related to the density of the peak latency. In a previous study related to the ulnar nerve¹⁴, no correlation was noted between these two indices; however, in the present tibial nerve,

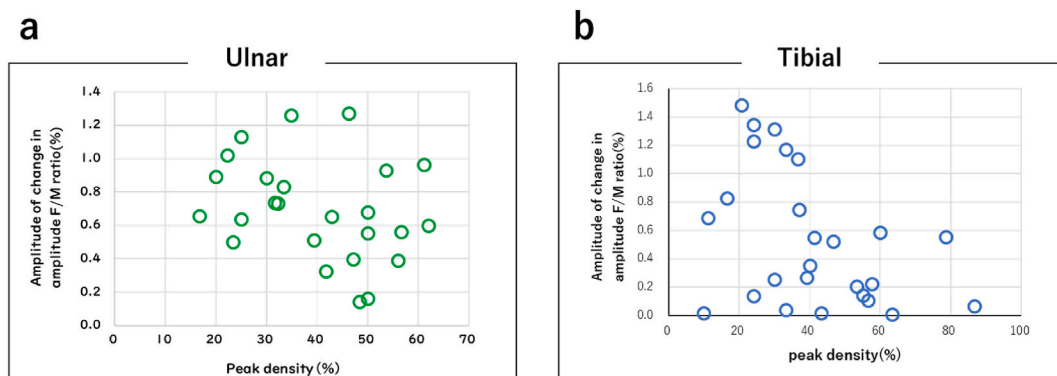


Fig. 7. Scatter plots between peak density and amplitude changes in the ulnar nerve and tibial nerve. (a) In the ulnar nerve, there is a group of subjects who show high amplitudes with the additive averaging process, regardless of the peak density. This is because the decrease in amplitude by the additive averaging process varies due to the class, which is specific to the upper limb in that a localized huge waveform appears. (b) In the tibial nerve, the effect of peak density is reflected more clearly by the appearance of high amplitude waveforms in a wide range. (*Ulnar figure was published in Journal of Neuroscience Methods, Vol 369, Marina Todo, Toshiaki Suzuki, Masaaki Hanaoka, Hitoshi Asai, A new waveform analysis method reflecting the diversity of F-wave Waveforms–Waveform types in healthy subjects based on the combined use of the additive averaging method and histograms-, Page 109474, Copyright Elsevier (2022).*).

only the negative peak showed a significant negative correlation. In other words, in the case of the tibial nerve, the peak density affected the amplitude of the additive averaging process. The factors that were only correlated with the tibial nerve were analyzed based on the characteristics of two scatter plots in Fig. 7. With regard to the ulnar nerve, there is a group of subjects who have high amplitudes with additive averaging processing, regardless of the peak density. This may be due to the unique waveform class in the upper limb, which has the appearance of a localized huge waveform, such as ulnar nerve class 3-1¹⁴). In this class, the huge waveforms cause the value of the average data to be large, but the additive averaging process cancels out the huge waveforms in a few cases. As a result, the value of the arithmetic mean data becomes smaller and the difference from the average data becomes greater.

The scatter plots in the present study reflect how dense the peak latency is in a certain interval and do not take into account the effect of the amplitude of the waveform obtained for each stimulus. In the case of the tibial nerve, the incidence of localized huge waveforms (like those of the ulnar nerve) was low. As a result, the effect of the amplitudes of individual waveforms on the amplitude decrease due to the additive averaging process was small, and the effect of peak density was more clearly reflected. However, in the positive peak, there was no correlation with the amplitude decrease. This may be due to the part of the waveform after the third phase (the second negative wave) that is not reflected in the peak density. The peak density is an index that indicates the number of waveforms that appear in the 0.5-msec period before and after the peak latency of one waveform obtained by the additive averaging process. The positive waves of other waveforms are canceled out by the waveform after the third phase, and the positive peak latency of the waveform after the additive averaging process cannot reflect the dense area of the raw waveform. As a result, the peak density of positive peaks is expected to be low. Alternatively, the positive peak during the additive averaging process may be increased due to the influence of waveforms of different duration, resulting in a lower amplitude. These results suggest that—in the case of the tibial nerve—the amplitude decrease due to the additive averaging process reflects the peak density of the negative peak.

4.2. Comparison of the waveform classes between the tibial and ulnar nerves

The histogram used to visualize the density of peak latency can be categorized into three classes in both the tibial nerve and the ulnar nerve. The major difference between the tibial and ulnar nerves was that there was no class with a localized huge waveform in the tibial nerve. The reason for this will be discussed by comparing the number of muscle fibers and motor units of the muscle from which the F wave is derived.

In the present study, the abductor hallucis muscle was used as the F wave conductor during tibial nerve stimulation; this muscle has 44953 muscle fibers, which is less than the 69565 fibers of the little finger abductor muscle used during ulnar nerve stimulation. In terms of the thickness of the muscle fibers, it has been reported that the abductor hallucis muscle is thicker than the little finger abductor muscle [15,16]. In other words, based on the thickness of the muscle fibers, we can expect the abductor hallucis muscle to be more likely to involve FF-type motor units, which are larger in size in terms of the motor unit type. As a result, we consider that the motor unit that constitutes the F wave derived from the abductor hallucis muscle involves a larger motor unit than the ulnar nerve, resulting in the appearance of a high-amplitude waveform. In the ulnar nerve, a huge waveform appears during synchronous firing or when a large motor unit fires in a waveform composed of small motor units. In contrast, in the tibial nerve, huge waveforms do not appear, while many waveforms with large amplitude generally appear; thus, no conspicuously huge waveforms are observed.

Another feature of the tibial nerve is that it is more complicated than the F wave, which can be measured from the upper limb. The abductor hallucis longus muscle has more motor units than the little finger abductor muscle [17], and more motor units are involved in the composition of the F wave than the ulnar nerve. In addition, the tibial nerve has a longer conduction distance in comparison to the ulnar nerve and the time is more variable, which is also a factor in its complexity.

In the case of the tibial nerve in this study, although there are various influencing factors, the waveforms recorded from healthy subjects could be categorized into four classes, which is a standard for future waveform analyses. The categorization of F waves class reflects muscle and spinal nerve function and will be pursued further by comparison with F waves in actual diseased patients. In addition to its use as an evaluation index for spasticity and voluntariness due to cerebrovascular disease, the F wave classification system can be used to non-invasively evaluate the neurophysiology of muscle weakness resulting from a decrease in motor units due to aging.

One limitation associated with this method is that the amplitude decrease due to the additive averaging process does not reflect the amplitude of each waveform. In the future, we hope to develop a waveform analysis method that reflects the neural-specific waveform shapes and amplitudes based on the categorization of F wave classes in healthy subjects obtained in this study.

5. Conclusion

We herein examined the relationship between the amount of amplitude decrease and peak density in the additive averaging process for F waves derived from tibial nerve stimulation and categorized the tibial nerve-specific types based on histograms. The results suggest that the peak density of negative peaks and the overlap of negative and positive peaks are involved in the amount of reduction in the amplitude by the additive averaging process. In addition, the type of diversity among healthy subjects could be divided into four categories based on the characteristics of the histogram.

Funding

This research was not supported by any funding sources.

Data availability statement

Data included in article/supp. material/referenced in article.

CRediT authorship contribution statement

Marina Todo: Formal analysis, Methodology, Project administration, Writing – original draft, Conceptualization. **Toshiaki Suzuki:** Project administration, Supervision, Conceptualization. **Masaaki Hanaoka:** Formal analysis, Methodology. **Hitoshi Asai:** Methodology, Supervision.

Declaration of competing interest

The authors declare that they have no known competing financial interests or personal relationships that could have appeared to influence the work reported in this paper.

Acknowledgments

We are grateful to all of the volunteers for participating in this study. We also thank International Journal of Neurorehabilitation and Journal of Neuroscience Methods for allowing us to cite their figures.

References

- [1] J. Kimura, N. Kohara, *Nerve Conduction and Electromyography Studies*, second ed., 2018, pp. 90–91. Tokyo, Japan.
- [2] E. Chroni, I.S. Tendero, A.R. Punga, et al., Usefulness of assessing repeater F-waves in routine studies, *Muscle Nerve* 45 (2012) 477–485, <https://doi.org/10.1002/mus.22333>.
- [3] A. Andreas, P. Karanasios, A. Makridou, et al., F-wave characteristics as surrogate markers of spasticity in patients with secondary progressive multiple sclerosis, *J. Clin. Neurophysiol.* 27 (2010) 120–125, <https://doi.org/10.1097/WNP.0b013e3181d64c94>.
- [4] T. Suzuki, E. Saitoh, M. Tani, et al., Characteristic appearances of the H-reflex and F-wave with increased stimulus intensity in patients with cerebrovascular disease, *Electromyogr. Clin. Neurophysiol.* 42 (2002) 67–70.
- [5] T. Suzuki, Y. Bunno, M. Tani, et al., F-wave waveform values based on the correlation coefficient of each waveform increased following improved voluntary movements in a patient with cerebrovascular disease: a case study with long-term follow-up, *Int. J. Neurorehabilitation* 3 (2019), 1000206.
- [6] E. Chroni, D. Veltsista, C. Papapavlou, et al., Generation of Repeater F waves in healthy subjects, *J. Clin. Neurophysiol.* 34 (2017) 236–242, <https://doi.org/10.1097/WNP.0000000000000360>.
- [7] S. Peioglou-Harmoussi, P. Fawcett, D. Howe, et al., F-responses: a study of frequency, sharp and amplitude characteristics in healthy control subjects, *J. Neurol. Neurosurg. Psychiatry* 48 (1985) 1159–1164, <https://doi.org/10.1136/jnnp.48.11.1159>.
- [8] A. Eisen, K. Odusote, Amplitude of the F-wave: a potential means of documenting spasticity, *Neurology* 29 (1979) 1306–1309, <https://doi.org/10.1212/wnl.29.9.part.1.1306>.
- [9] T. Komori, R. Takahashi, K. Hirose, et al., The significance of F-wave negative peak for clinical application, *Jpn. J. Electroencephalogr. Electronmyogr.* 17 (1989) 255–262.
- [10] T. Komori, R. Takahashi, K. Hirose, et al., F-wave analysis using signal averaging as a simple and reliable method, *Jpn. J. Electroencephalogr. Electronmyogr.* 18 (1990) 293–301.
- [11] H. Hiratsuka, T. Kawai, M. Kawai, et al., Comparison of F wave and H wave on spastic hand, *Orthop. Traumatol.* 35 (1986) 237–239.
- [12] S. Sakamaki, T. Takasu, *Clinical and electrophysiological study of patients with prolonged F wave duration*, *Clinical electroencephalography.* 30 (1988) 7–11.
- [13] M. Todo, T. Suzuki, H. Asai, Comparison of F-wave amplitudes between addition average mean processing and mean value processing, *Rigakuryoho Kagaku* 36 (2021) 1–7.
- [14] M. Todo, T. Suzuki, M. Hanaoka, H. Asai, A new waveform analysis method reflecting the diversity of F-wave Waveforms—Waveform types in healthy subjects based on the combined use of the additive averaging method and histograms-, *J. Neurosci. Methods* 369 (2022), 109474, <https://doi.org/10.1016/j.jneumeth.2022.109474>.
- [15] T. Ajiri, A comparative study on muscle fiber organization in human hand muscles, *J. Showa Med. Assoc.* 41 (1981) 693–706.
- [16] H. Nakanishi, Studies on myofibrous organization of intrinsic muscles in human foot, *J. Showa Med. Assoc.* 41 (1981) 707–716.
- [17] C. Neuwirth, S. Nandedkar, E. Stalberg, et al., Motor unit number index (MUNIX): a novel neurophysiological marker for neuromuscular disorders; test-retest reliability in healthy volunteers, *Clin. Neurophysiol.* 122 (2011) 1867–1872, <https://doi.org/10.1016/j.clinph.2011.02.017>.